Claridge E, Preece SJ (2003) An inverse method for the recovery of tissue parameters from colour images. *Information Processing in Medical Imaging* (IPMI), Taylor C and Noble JA (Eds.) LNCS 2732, 306-317. Springer.

An inverse method for the recovery of tissue parameters from colour images

Ela Claridge and Steve J Preece

School of Computer Science, The University of Birmingham, Birmingham B15 2TT, U.K.
{e.claridge s.j.preece}@cs.bham.ac.uk

Abstract. The interpretation of colour images is presented as an inverse problem in which a mapping is sought between image colour vectors and the physiological parameters characterizing a tissue. To ensure the necessary one-to-one correspondence between the image colours and the parameters, the mapping must be unique. This can be established through testing the sign of the determinant of the Jacobian matrix, a multi-dimensional equivalent of a discrete derivative, over the space of all parameter values. Furthermore, an optimisation procedure is employed to find the set of filters for image capture which generate image vectors minimizing the mapping error. This methodology applied to interpretation of skin images shows that the standard RGB system of filters provides for a unique mapping between image values and parameters characterizing the normal skin. It is further shown that an optimal set of filters reduces the error of quantification by a factor of 2, on average.

1 Introduction

Recently Cotton and Claridge proposed a novel approach to the interpretation of colour medical images [1]. It is based on the hypothesis that, because colours seen at the surface of a tissue reflect its internal structure and composition, it should be possible to recover this information from colour images of the tissue. This approach was successfully applied to skin imaging [2] and early clinical trials show its value in melanoma diagnosis [3].

The method consists of a modelling step, which needs to be carried out only once, and an interpretation step. In the first step a predictive mathematical model of tissue coloration is constructed. It requires data on the tissue's laminar structure, the optical properties of the layers and an appropriate model of radiation transport. Given a specific set of tissue parameters, such as the thickness of the layers and the concentration of all the pigments, a radiation transport model computes a corresponding spectrum. Image vectors corresponding to a given image acquisition system are then obtained by convolving the spectrum with the appropriate RGB filter response curves. From the knowledge of physiology, the normal ranges for all the tissue parameters can be established and RGB image vectors computed for all combinations of the parameters. In this way a cross-reference between histology and colour, a model of colouration, is obtained. Provided that the mapping is unique, two-

Claridge E, Preece SJ (2003) An inverse method for the recovery of tissue parameters from colour images. *Information Processing in Medical Imaging* (IPMI), Taylor C and Noble JA (Eds.) LNCS 2732, 306-317. Springer.

way predictions are possible: from tissue composition to its colour; and, importantly, from the tissue colour to its composition.

In the second step, the model of colouration is employed to interpret colour images of tissue. If tissue parameters are in the normal ranges, the corresponding colour will have its entry in the model and hence its histological parameters can be obtained. New images called parametric maps are constructed by reading the colours from the original image point by point, obtaining the tissue parameters from the model, and recording the magnitude of each parameter at the corresponding location of a respective parametric map. Instances of abnormal tissue constituents can be identified as they lie outside the range of colouration predicted by the model. Their parametric maps can also be constructed and be a subject of further interpretation.

In the context of skin imaging, the method computes parametric maps depicting the concentration of epidermal melanin and dermal blood, the concentration of dermal melanin, if present, and the thickness of the papillary dermis. Figure 1 shows an image of a lesion (a melanoma) and the four parametric maps. Clinical features, related to physiology, are easy to detect in these maps. A stepwise diagnostic procedure using combinations of the features results in melanoma detection with 80.1% sensitivity and 82.7% specificity on a set of 348 lesions [3], which compares very well with other diagnostic methods.

(a) (b) (c) (d) (e)

Fig. 1.. (a) A colour image of a melanoma together with parametric maps showing: (b) total melanin (darker = more); (c) dermal melanin, whose presence suggests abnormality (brighter = more); (d) papillary dermis showing the collagen hole and peripheral increase (brighter = more); (e) dermal blood showing the absence in the centre and increase on the periphery (darker = more). These features are typical for melanoma and can be easily seen in the maps

One of the key factors on which the success of this method depends is the uniqueness of mapping between the tissue parameters and the image values. Cotton and Claridge's justification of this fact is informal and it relies on a particular geometric distribution of image vectors in RGB colour space [1]. This paper develops the theoretical underpinnings for that work. The original approach is re-presented in the context of inversion methods used in optical tomography. This paper proposes a formal generic method for determining the uniqueness of mapping between tissue parameters and image vectors, which is the necessary condition for any inversion method. It then demonstrates that the RGB image vectors used in Cotton and Claridge's work indeed provide a unique inverse solution. The paper shows further how to determine the optimal set of filters which minimise the uncertainty in quantification of tissue parameters. The optimal set of filters is computed for the normal skin and shown to reduce the error of quantification by a factor of 2 on average in comparison to standard RGB filters.

Claridge E, Preece SJ (2003) An inverse method for the recovery of tissue parameters from colour images. *Information Processing in Medical Imaging* (IPMI), Taylor C and Noble JA (Eds.) LNCS 2732, 306-317. Springer.

2 Finding Tissue Parameters as an Inversion Process

Deriving tissue parameters from a model of tissue colouration is akin to the inverse solution approach used in optical modelling and reconstruction ([4], abstract):

> "*Given a set of measurements of […] light […] on the surface of the object, there exists a unique three-dimensional distribution of internal scatterers and absorbers which would yield that set. Thus imaging becomes a task of solving an inverse problem using an appropriate model of photon transport.*"

In the context of this work, light measurements are available in the form of image vectors (e.g. [r g b]) and the solution sought is reduced to finding a two-dimensional distribution of scatterers and absorbers projected onto the surface. Importantly, the inversion method must provide a solution which is unique. In addition, to be of practical use, the solution has to be accurate enough for the intended clinical application. The uniqueness is an objective criterion and its existence can be formulated mathematically. The notion of "sufficient accuracy" is highly subjective and depends on the needs of the application domain. However, it is possible to replace it with a weaker condition which is amenable to mathematical treatment, namely that the error of estimation is at is minimum according to a given objective criterion.

3 Image Formation as a Two-step Mapping

For the purpose of this study the image formation process is presented as a sequence of two steps. In the first step the incident light interacts with an object. As a result of this interaction any remitted light has its spectrum altered depending on the object composition. In the second step, an image acquisition device captures and integrates specific portions of the remitted spectra and generates a single value corresponding to each spectral band. The result of collating all the bands is a pixel vector such as, for example, a typical [r g b] 3-dimensional vector. This process can be expressed mathematically as follows. Let

$$\mathbf{p} = \{p_k\}_{k=1,\ldots,K}\ ,\ \mathbf{p} \in P \tag{1}$$

be a vector of k parameters which affect the object colouration, and P is the space of all possible parameter variations associated with a given object. A spectrum is represented by a set of values λ_m at a number of discrete wavelengths m

$$\lambda = \{\ \lambda_m\ \}_{m=1,\ldots,M},\ \lambda \in \Lambda \tag{2}$$

and the space Λ defines all possible spectra that can be remitted from a given object. Image values captured by a camera with N optical filters are represented by a vector

$$\mathbf{i} = \{i_n\}_{n=1,\ldots,N}\ ,\ \mathbf{i} \in I \tag{3}$$

where I describes the space of all possible image values corresponding to parameters $\mathbf{p} \in P$.

The mapping *a* defined as

$$a : P \rightarrow \Lambda \tag{4}$$

represents the first step in the imaging process, denoting a function from parameter space to wavelength space. This mapping produces the spectral reflectance λ for a given parameter vector **p**. The second step, i.e. the digital image capture, is represented by the mapping function *b*

$$b : \Lambda \rightarrow I \tag{5}$$

In real imaging *b* is a mapping from the continuous space of spectra and is implemented by optical filtering. In discrete form *b* is a convolution of λ with a filter response function R. The function for the n-th filter can be defined as

$$i_n = \sum_{m=1}^{M} R_m^n \lambda_m \tag{6}$$

The matrix $[R_m^n]$ defines a set of filter response functions. For physically realisable filters all values R_m^n are positive.

The entire process of image formation can be represented by a two-step function *f*

$$f = a \circ b \quad f : P \rightarrow I \tag{7}$$

which describes the correspondence between specific parameters characterising the tissue and the pixel vector captured through a given set of optical filters.

4 Finding the Inverse Solution

In terms of the framework introduced above, the aim of estimating the parameters which characterise a tissue from its colour (or more generally from its multi-spectral) image is to find an inverse function

$$f^{-1} : I \rightarrow P \tag{8}$$

such that *f* defines a unique, one-to-one mapping between the points in P and the points in I and $\mathbf{p} = f^{-1}(\mathbf{i})$ exists for all $\mathbf{p} \in P$. The solution will be sought by, first, specifying a forward mapping *f* and then testing its uniqueness. The first component of the mapping function, *a*, will take the form of a photon transport model, computing a spectrum corresponding to a given parameter vector. At this stage the function *b*, applying a set of filters to the spectra generated by *a*, will be assumed to be known. The uniqueness of mapping for *f* will be tested by examining the behaviour of the determinant of the Jacobian matrix over all $\mathbf{p} \in P$. Next, the restriction on *b* will be removed and an optimization scheme will be applied to select a set of N filters such that $f : P \rightarrow \Lambda \rightarrow I$ is unique and the error of mapping is at its minimum.

4.1 Generative model of colouration: forward mapping

In order to perform mapping *a*, it is necessary to have either a mathematical model which can predict spectral reflectance for a given set of parameter values, or some technique for measurement of the appropriate spectra. Mathematical models provide a

solution to the radiative transfer equation at a number of discrete wavelengths and can be implemented as either deterministic or stochastic algorithms. Deterministic algorithms include a Kubelka-Munk approximation [9] and radiative transfer equation (in [4], p842); the most common stochastic method is Monte Carlo simulation [5].

The input parameters required by the algorithms of either class can be subdivided into those which characterise the entire tissue type and those which characterise a specific instance of the tissue. The first group typically includes absorption and scatter coefficients and the second group includes variable factors such as thickness of tissue layers and concentrations of absorbing compounds. Function *a*, which effectively implements a solution to a radiative transfer equation, operates on the parameters of the second group whereas parameters of the first group are treated as constants.

To test the uniqueness of mapping of *a* and, later on, to seek the optimal *b* which minimises the mapping error, it is necessary to ensure that the parameter space P covers the *entire* range of histologically valid concentrations and thicknesses. P has also to be appropriately discretised. The outline of the algorithm is as follows:

```
given
 incident light
 absorption and scatter coefficients for all the components
 the spatial arrangement of the components
for all concentrations and thicknesses of parameter p1
 for all concentrations and thicknesses of parameter p2
    . . .
      for all concentrations and thicknesses of parameter pK
        compute λ = a( p1, p2, ..., pK )
```

The image vectors **i** corresponding to the spectra λ obtained above are computed by convolving each spectrum with a set of filter response functions, typically RGB.

4.2 Testing for Uniqueness of the Solution

Finding a unique vector of parameters **p** corresponding to a given image vector **i** corresponds to finding a unique solution to the equation

$$\mathbf{p} = f^{-1}(\mathbf{i}) \tag{9}$$

In one-dimensional case, i.e. when *f* is a single-valued function on a single variable, one-to-one correspondence is ensured if and only if *f* is monotonic on the entire domain P of **p**. Mathematically this can be expressed as

$$\left|\frac{df}{dp}\right| > 0 \quad \forall\, \mathbf{p} \in P \tag{10}$$

Drawing on differential geometry, the inverse function theorem [6] enables us to derive an equivalent condition for the case when *f* is a (discrete) vector valued function of a vector variable. Jacobian matrix defined as

$$J = \begin{bmatrix} \frac{\partial f_1}{\partial p_1} & \frac{\partial f_1}{\partial p_2} & \cdots & \frac{\partial f_1}{\partial p_k} \\ \cdots & \cdots & \cdots & \cdots \\ \frac{\partial f_n}{\partial p_1} & \frac{\partial f_n}{\partial p_2} & \cdots & \frac{\partial f_n}{\partial p_k} \end{bmatrix} \tag{11}$$

is a multi-dimensional equivalent of the one-dimensional derivative. The inverse function theorem states that if the determinant of the Jacobian matrix, det(J), is non-zero at a point $\mathbf{p} = \mathbf{p}_0$ then there exists a neighbourhood around $\mathbf{p}_0$ where f can be approximated linearly. It follows then that within this neighbourhood there is one-to-one mapping between $\mathbf{p} \in P$ and $\mathbf{i} = f(\mathbf{p}) \in I$. The condition

$$\det(J) \neq 0 \ \forall \ \mathbf{p} \in P \tag{12}$$

is necessary but insufficient if P is discrete, because there may be instances of $\mathbf{p}$ not in P where f has "turning points" – local extrema. Such points are characterised by the change of sign in det(J). If det(J) has the same sign over the whole domain P, f does not have any local extrema and thus is monotonic over the whole domain of P. Thus to ensure the uniqueness of mapping over the whole of P we require that the determinant of the Jacobian matrix is either strictly positive or strictly negative for all $\mathbf{p} \in P$. Then there exists a neighbourhood around each $\mathbf{p} \in P$ where there is one-to-one mapping between parameters $\mathbf{p}$ and image vectors $\mathbf{i}$. Within such neighbourhood the inverse function f^{-1} can be expressed as

$$d\mathbf{p} = J^{-1} \, d\mathbf{i} \tag{13}$$

where $d\mathbf{p} = \mathbf{p} - \mathbf{p}_0$ and $d\mathbf{i} = \mathbf{i} - \mathbf{i}_0$, $\mathbf{i}_0 = f(\mathbf{p}_0)$.

4.3 Finding Optimal Filters

The uniqueness conditions formulated above ensure that for a given image vector $\mathbf{i}$ and a given function f there is a unique set of corresponding parameters $\mathbf{p}$ characterising the tissue at the specific image location. In practice mapping f is not error free and even when in theory the following is true

$$f^{-1}(\mathbf{p}_j) \neq f^{-1}(\mathbf{p}_k) \quad \text{for } j \neq k, \tag{14}$$

a camera digitisation error σ_{cam} can be such that $| f^{-1}(\mathbf{p}_j) - f^{-1}(\mathbf{p}_k) | < \sigma_{cam}$ and it is impossible to distinguish $\mathbf{p}_j$ and $\mathbf{p}_k$. In this situation only the requirements of a specific application domain can determine what level of uncertainty makes the parameter recovery clinically useful.

Although it is not possible to find a generic criterion for the level of uncertainty, it is possible to find a criterion for finding a mapping which minimizes a mapping error. Drawing on the definition of $f = a \circ b$, it can be seen that whereas a is determined by the physics of image formation, b can be decided by the user. Specifically, by varying the filters, the mapping error can be varied also.

The two main sources of error are the uncertainties in the absorption and scatter coefficients (σ_{spec}) and the camera digitisation error (σ_{cam}). σ_{spec} captures a mainly

experimental error and is commonly available, together with the coefficient data (e.g. as the standard deviation at each wavelength [10]). Spectral errors associated with each parameter vector **p** are then calculated using standard error propagation. Partial derivatives $\partial p/\partial i$ are obtained from J^{-1}. From statistical error analysis [7]

$$\sigma_{spec} = \sum_k \left(\sum_n \frac{\partial p}{\partial i} \sigma_{i_n}^2 \right)^{1/2} \quad (15)$$

The second error, σ_{cam}, is derived from the camera SNR and is also wavelength dependent. Using statistical error analysis it is possible to estimate the error from each source for a given p_k (for details see [8]). As the two sources are independent, the respective errors can be combined to give the overall error estimate

$$\sigma_{pk} = \sqrt{\sigma_{spec}^2 + \sigma_{cam}^2} \quad (16)$$

It is now possible to define an optimisation scheme which selects a set of N filters such that the mapping between **p** and **i** is unique for all $\mathbf{p} \in P$ and that the error of mapping (16) is minimised. A typical optical filter can be defined, for example, by the central wavelength (CW) and full width at half maximum (FWHM). For N filters this defines an N x 2 search space. The use of the Jacobian to test the existence of the unique solution requires the computation of the image vector, $\mathbf{i} = f(\mathbf{p}) = b(\, a(\mathbf{p})\,)$ and in practice filter response functions are represented in the form of a matrix $[R_m^n]$ (see equation (6)). The outline of the optimization algorithm is as follows:

```
until the stopping criterion is met
1. define a new set of filters R_m^n (defined by CW & FWHM)
2. for a given set of filter response functions R_m^n
      for each point p within a discretised parameter space
        compute the image vector i = b(R_m^n, a(p))
3. check that the Jacobian is either strictly positive or
   strictly negative for ALL the points p
      if true
        compute the inverse Jacobian matrix
      if false, return to step 1
4. compute the error of parameter recovery and use it to compute
   a stopping criterion.
```

5 Applying Methodology to Skin Imaging – Procedure and Results

The above analysis is now applied to the problem of computing quantitative parameters characterising the normal human skin from colour images. Earlier work by Cotton and Claridge showed the feasibility of deriving such parameters using a model of image formation [1], and also the clinical utility of the resulting parameteric maps in early diagnosis of melanoma [3]. In this paper we demonstrate that the derived histological parameters have one-to-one correspondence to RGB image vectors. We show further that the error in recovered parameter values can be reduced by selecting filters optimised for the specific set of skin parameters.

Claridge E, Preece SJ (2003) An inverse method for the recovery of tissue parameters from colour images. *Information Processing in Medical Imaging* (IPMI), Taylor C and Noble JA (Eds.) LNCS 2732, 306-317. Springer.

5.1 Optical Model of the Normal Skin

The skin is modelled as a two-layer structure. The optical characteristics of the upper layer, epidermis, are determined by a pigment melanin which strongly absorbs light in the blue range of the spectrum. Any light which is not absorbed enters the next layer, the dermis. A proportion of light is absorbed there by haemoglobin and oxyhaemoglobin in the blood, but most is scattered by collagen back towards the skin surface. On the way back light is absorbed again by melanin in the epidermis and what remains is remitted and registered by a camera. Absorption coefficients for melanin and haemoglobin and scatter coefficients for dermal collagen are the constants in the modelling process. The variable quantities are the concentration of melanin, concentration of blood pigments and thickness of the papillary dermis, making the dimension of the parameter space P to be 3.

The spectra corresponding to the histologically valid parameter values characterising melanin and blood were computed using Kubelka-Munk theory [9]. Monte Carlo simulations return virtually the same spectra, but they are much more time consuming. The absorption and scatter coefficients were taken from published data [10]. Parameter ranges for melanin, blood and papillary dermis were discretised to define respectively 10 x 10 x 4 spectra. This choice of discretisation was arbitrary, but additional experiments showed that it did not affect the results of the uniqueness test. Figures 2a-c show the changes in the remitted spectrum effected by changes in the levels of melanin, the blood pigments and thickness of the papillary dermis.

5.2 Testing One-to-one Mapping for RGB Filters

Each spectrum generated above was convolved with the R, G and B filter (CW=610nm, 550nm and 450nm respectively; FWHM=60) yielding 10 x 10 x 4 image vectors, $\mathbf{i} = f(\mathbf{p})$ corresponding to 10 x 10 x 4 parameters $\mathbf{p} = [p_{mel}, p_{haem}, p_{papd}]$. The det(J) was positive for every $\mathbf{p}$, thus showing the uniqueness of mapping between the parameters and the image vectors for the RGB filters. This result confirms an earlier insight based on geometric interpretation of the mapping [1], that the parameters can be derived uniquely from RGB image values. Parametric maps based on RGB filters have already been validated on a large data set of 348 lesions [3].

5.3 Computing Optimum Filters

The standard RGB filters produce parametric images which provide the clinician with diagnostically important information about the state of the skin. However, there may exist combinations of filters which further decrease the uncertainty of mapping. To define filters which minimise the mapping error, an optimisation procedure was implemented following the algorithm in section 4.3. A genetic algorithm (GA) provided in MATLAB Statistic Toolbox was used to drive the optimisation.

Three filters are required for the unique mapping of three parameters. Each filter is defined by two parameters, the central wavelength and FWHM, thus defining a 6-dimensional search space. The search space was constrained so that a filter has to lie

entirely within the visible part of the spectrum (400-700nm) and its FWHM must be within the range 25-100nm. The fitness function for the GA computations was defined as a reciprocal of the sum of the camera and the spectral errors. The GA was initialised using random seeds and run 5 times to ensure that the results were not dependent on the starting values.

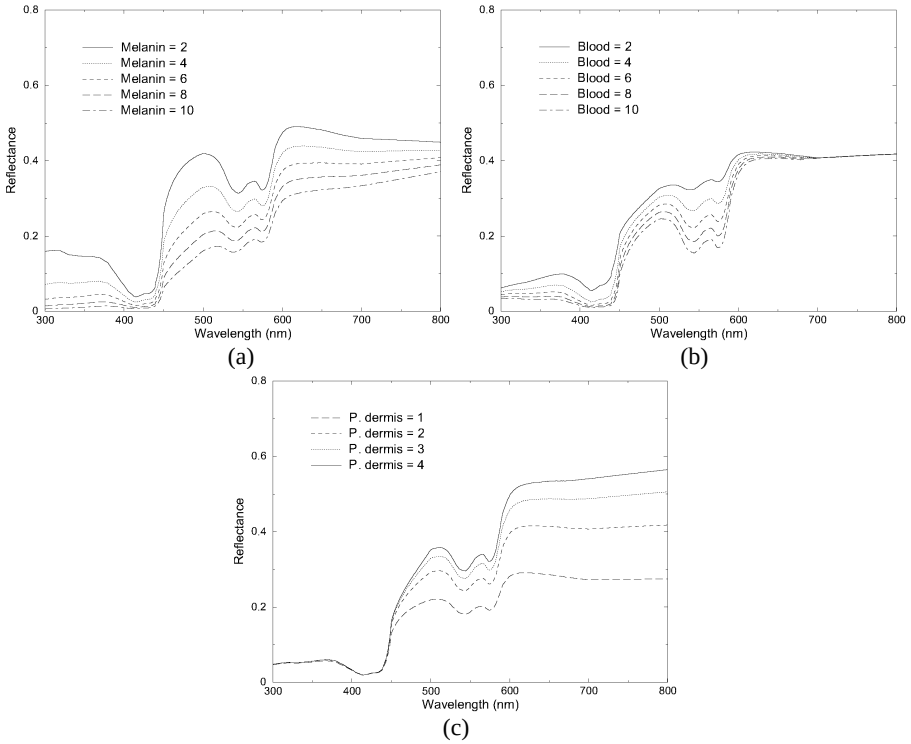

Fig. 2. Remittance spectra of the normal human skin (a) for varying melanin concentration; (b) for varying blood concentration (oxy- and de-oxyhaemoglobin in equal proportions); (c) for varying thickness of the papillary dermis

5.4 Results and Discussion

The results of the runs were fairly consistent and returned the filter parameters as shown in Table 1. The combined spectral and camera error (equation 16) associated with the recovery of melanin, blood and papillary dermis parameters was computed for several combinations of these parameters. Tables 2, 3 and 4 show typical errors for the optimal filters. The errors lie in the range 0.18-0.94 for melanin, 0.25-1.16 for blood and 0.07-0.14 for papillary dermis. Errors for the RGB filters (not shown here in full because of lack of space) vary between 0.35 and 1.8 for melanin, 0.6 and 1.6 for blood and 0.07 and 0.35 for papillary dermis.

Claridge E, Preece SJ (2003) An inverse method for the recovery of tissue parameters from colour images. *Information Processing in Medical Imaging* (IPMI), Taylor C and Noble JA (Eds.) LNCS 2732, 306-317. Springer.

Table 1. Filter parameters returned by the optimisation procedure.

Filter	CW (nm)	FWHM (nm)
1	485 ± 0.75	24 ± 0.90
2	560 ± 0.73	14 ± 0.55
3	700 ± 0.01	95 ± 0.72

Table 2. Error in recovery of melanin level for the fixed thickness of the papillary dermis (level 2) and varying levels of melanin and blood. Every other level is shown. Error is relative to melanin level, e.g. for melanin level 4 and blood level 2, the recovered melanin level is 4±0.23

Blood level	Melanin level				
	2	4	6	8	10
2	0.21	0.23	0.25	0.28	0.30
4	0.28	0.31	0.34	0.37	0.40
6	0.37	0.41	0.45	0.49	0.53
8	0.49	0.54	0.59	0.64	0.70
10	0.66	0.72	0.79	0.86	0.94

Table 3. Error in recovery of blood level for the fixed thickness of the papillary dermis (level 2) and varying levels of melanin and blood. Every other level is shown. Error is relative to blood level, e.g. for melanin level 4 and blood level 2, the recovered melanin level is 2±0.35

Blood level	Melanin level				
	2	4	6	8	10
2	0.29	0.35	0.42	0.51	0.62
4	0.34	0.41	0.49	0.60	0.73
6	0.39	0.48	0.58	0.70	0.85
8	0.46	0.56	0.67	0.82	0.99
10	0.54	0.65	0.79	0.96	1.16

Table 4. Error in recovery of papillary dermis thickness level for a fixed thickness of the papillary dermis (level 2) and varying levels of melanin and blood. Every other level is shown. Error is relative to the papillary thickness level, e.g. for melanin level 4 and blood level 2, the recovered thickness level for papillary dermis level is 2±0.074

Blood level	Melanin level				
	2	4	6	8	10
2	0.073	0.074	0.075	0.075	0.076
4	0.079	0.080	0.081	0.082	0.082
6	0.086	0.087	0.088	0.089	0.089
8	0.094	0.095	0.096	0.098	0.107
10	0.102	0.109	0.119	0.130	0.141

It is interesting to analyse the choice of optimal filters by relating them to the graphs showing the variability of the individual parameters (figure 2). A fairly broad filter centered at 700nm is a clear choice for the papillary dermis thickness. At this wavelength variations related to blood and melanin are much smaller in comparison to variations related to papillary dermis. A filter centered at 560nm corresponds to a range of wavelengths where sensitivity to change in blood level is very high; e.g. the peak absorption for oxyhaemoglobin is at 558nm. The first filter, at 485nm, coincides

with the maximum variability related to melanin levels and it carefully avoids encroaching on the higher range of wavelengths where variability in blood levels begins to show.

The comparison of error levels for the optimal filters and the RGB filters shows clearly the advantage of carefully tuning the spectral parameters of the imaging system. It could be argued that the above comparison is somewhat unfair with respect to the actual working solution for the skin imaging which uses one near-infrared filter to estimate the thickness of the papillary dermis in addition to three RGB filters for quantification of the remaining two parameters. Bearing in mind that the optimization process constrained the filters to lie within the range between 300 and 700 nm, it is very likely that filter 3, currently at the top of this range at 700nm, would by placed further towards infra-red. In another study [11] the authors sought to find a set of filters which would optimise recovery of melanin and blood only, assuming a known thickness of the papillary dermis. That work showed that using just two optimal filters error reduction up to 20% can be achieved in comparison to the standard RGB filters.

6 General Discussion

This paper makes several contributions in the area of medical image interpretation. In terms of methodology, it shows that an existing scheme [1] for derivation of tissue parameters from colour images can be viewed as a subset of optical reconstruction methods [4]. Within this framework the problem of finding a mapping between image colours and tissue parameters is formulated in terms of finding a unique inverse solution, given the forward mapping derived from the physical model of image formation. Specifically, the solution involves computing the Jacobian matrix of partial derivatives of image values with respect to parameters characterizing the tissue. A simple test is used to establish the uniqueness of the mapping. Once this condition is confirmed, the inverse mapping can be implemented in a number of ways. This approach is generic and is the main contribution of this paper. In addition, by formulating the mapping as a two step process, it is possible to find the optimal set of filters which minimize the mapping error.

Although the method is not tomographic, it is capable of producing parametric maps which show the surface distribution and the magnitudes of individual tissue components. The depth resolution is poor, being limited by both absorption and scatter. Within-the-surface resolution varies depending on scatter, so that small details are not always resolved. However, the maps showing gross (low-passed) distribution of parameters are still likely to give useful diagnostic insight into the tissue properties.

The methodology involved and the nature of results are similar to quantitative spectroscopy. The main difference is that information is shown in the form of an image, capturing not only quantitative data, but also spatial patterns and relationships. The recently developed fNIR imaging [12] is similar in this respect. Interpretation of hyperspectral images is also likely to benefit from the ability to find the spectral bands specifically optimized for a task in hand. The selection of optimal filters is carried out only once, prior to data acquisition and from there on images can be

Claridge E, Preece SJ (2003) An inverse method for the recovery of tissue parameters from colour images. *Information Processing in Medical Imaging* (IPMI), Taylor C and Noble JA (Eds.) LNCS 2732, 306-317. Springer.

acquired using a standard camera equipped with a small number of optical filters. This reduces cost, storage and computational requirements.

7 Conclusions

This work has laid down the foundations for a generic image interpretation method which allows one to compute histologically based parameters characterizing epithelial tissues. Given the optical characteristics of the tissue components and their laminar structure, it is now possible to establish, thorough a formal analysis, whether a unique correspondence exists between the tissue parameters and its colours. When this condition is met, the method can estimate tissue composition from optical images captured through a small number of filters chosen to optimize the parameter recovery. A substantial body of experimental work on skin imaging showed that the method offers a unique in-vivo insight into the tissue structure and can improve diagnosis. The theory presented in this paper should enable this kind of analysis to be readily extended to other imaging domains, including other epithelial tissues. Indeed, ongoing work on ocular fundus and colon imaging shows that this is the case.

References

1 Cotton SD, Claridge E, Hall PN. Noninvasive skin imaging, Information Processing in Medical Imaging (LNCS 1230) (1997) 501-507
2 Claridge E, Cotton S, Hall P, Moncrieff M. From colour to tissue histology: Physics based interpretation of images of pigmented skin lesions. Medical Image Computing and Computer-Assisted Intervention - MICCAI'2002. Dohi T and Kikinis R (Eds). LNCS 2488, vol I : Springer (2002) 730-738
3 Moncrieff M, Cotton S, Claridge E, Hall P. Spectrophotometric Intracutaneous Analysis: a new technique for imaging pigmented skin lesions. Br J Derm 146(3) (2002) 448-457
4 Arridge S, Hebden J. Optical imaging in medicine: II. Modelling and reconstruction. Phys Med Biol 42 (1997) 841-854
5 Prahl SA et al. A Monte Carlo Model of light propagation in tissue. SPIE Institute Series IS 5 (1989) 102-111
6 Lipschutz MM. Differential Geometry: McGraw-Hill (1969)
7 Kendall MG, Stuart A. The Advanced Theory of Statistics. Volume 1: Distribution Theory (3rd Ed): Charles Griffin & Co (1969)
8 Preece SJ, Claridge E. A technique for the geometry insensitive recovery of parameters which characterise human skin. Journal of the Optical Society of America (submitted)
9 Egan WG, Hilgeman TW. Optical Properties of Inhomogeneous Materials: Academic Press (1979)
10 Anderson R, Parrish BS, Parrish J. The optics of human skin. The Journal of Investigative Dermatology 77(1), 13-19 (1981).
11 Preece SJ, Claridge E. Physics-based quantitative image interpretation using material specific spectral characterisation models. IEEE Pattern Analysis and Machine Intelligence (submitted)
12 Hoshi Y, Chen SJ, Tamura M Spatiotemporal imaging of human brain activity by functional near-infrared spectroscopy. American Laboratory 33 (20) 35-39 (2001)